J Mater Sci (2014) 49:3080–3098
DOI 10.1007/s10853-013-8010-5

Chain flexibility versus molecular entanglement response to rubbing deformation in designing poly(oxadiazole-naphthylimide)s as liquid crystal orientation layers

Andreea Irina Barzic · Radu Dan Rusu · Iuliana Stoica · Mariana Dana Damaceanu

Received: 18 October 2013 / Accepted: 30 December 2013 / Published online: 14 January 2014

Abstract Four poly(oxadiazole-imide)s containing naphthalene rings, with different flexibility and molecular weight, are investigated with respect to their rheological properties to establish the optimal processing conditions from solution phase to film state for liquid crystal orientation purposes. The film uniformity and strength are determined by monitoring the flow behavior and chain entanglements. The solution rheological data are in agreement with film tensile testing, revealing that higher molecular weight favors chain entanglements and implicitly the film mechanical resistance. In order to analyze the suitability of these films as alignment layers their surface is patterned by rubbing with two types of velvet. Liquid crystal alignment of 4′-pentyl-4-biphenylcarbonitrile nematic is tested by polarized light microscopy. The resulting behavior is correlated with the polyimide malleability and characteristics of the textile fibers, namely their polarity, size, and mechanical features. The competitive effects between chain flexibility and entanglements, together with the interactions occurring between the polymer and velvet are analyzed in order to explain the surface regularity, which influences the uniformity of the liquid crystal alignment. The contrast between dark and bright states recorded on the liquid crystal cell indicates that some of these polynaphthalimides are promising candidates for liquid crystal display devices.

A. I. Barzic (✉) · R. D. Rusu · I. Stoica · M. D. Damaceanu
"Petru Poni" Institute of Macromolecular Chemistry,
41A Grigore Ghica Voda Alley, 700487 Iasi, Romania
e-mail: irina_cosutchi@yahoo.com

A. I. Barzic
Faculty of Physics, "Alexandru Ioan Cuza" University,
11 Carol I Bdv, 700506 Iasi, Romania

Introduction

Among the high-performance polymers, aromatic polyimides (PIs) are particularly attractive for their outstanding thermal stability and good mechanical properties and usually used as high-performance engineering plastics [1, 2]. However, most of these PIs are neither soluble nor fusible because of the high rigidity and conjugation of their backbone [3]. High rigidity and conjugation of the PI backbone are responsible for high chemical and thermal stability, and high glass transition temperature, but at the same time these aspects contribute to poor solubility in organic solvents. Hence, there are some difficulties in fabrication, which may limit their applications, especially in the form of films, coatings, or fibers. So far, major effort has been devoted to synthesizing soluble PIs in organic solvents, while preserving their good thermal stability. Some methods have been put forward to improve their solubility. One of the successful approaches to overcome these deficiencies without sacrificing high thermal stability is the introduction of bulky, packing-disruptive groups in the polymer backbone or as side groups [4], the incorporation of flexible chains [5], or insertion of meta-oriented or asymmetrically substituted monomers [6].

From the variety of chemical structures reported in literature, it was found that polynaphthalimides have superior chemical and thermal stabilities compared to the more common five-membered ring PIs [7–10]. Other studies show that aromatic polyimides containing 1,3,4-oxadiazole ring in the main chain exhibit high thermal resistance in oxidative atmosphere, good hydrolytic stability, low dielectric constant, and tough mechanical properties [11]. In addition, the 1,3,4-oxadiazole ring, due to its electron-withdrawing character can facilitate the attraction and transport of electrons, making the corresponding polymers

very interesting for optoelectronic domain [12]. The combination of these structural modifications, that is, the incorporation of 1,3,4-oxadiazole rings, naphthalene units and flexible groups in the polymer backbones, minimizes the trade-off between the processability and basic properties of wholly aromatic PIs.

In most technological applications, PIs are utilized under the form of coatings or films, generally shaped from molten state or solution. As a consequence, the rheological properties in the incipient phase strongly influence the reliability and the features of the final product. For instance, the construction of liquid crystal display (LCD) devices involves introduction of PI films as liquid crystal (LC) alignment layers (ALs) with high transparency and specific topography [13]. The morphology of the PI films strongly depends on the microstructure, chain interactions, and processing conditions. Viscosity of the AL is an important product parameter because it determines AL thickness and uniformity during film casting on substrates or spin coating. Therefore, producers of AL have established manufacturing procedures that require the measurement of solution viscosity during production to insure product quality. Periodic samples are taken off-line to an analytical laboratory where viscosity is determined under controlled conditions. Also, the viscoelastic character of polymer solution reflects the entangled microstructure affecting flow stability and development of some crucial properties, such as dimensional stability, uniformity, and flexibility of the resulting AL.

On the other hand, it is necessary to adapt the AL surface to produce a homogeneous alignment of the LC. One of the most used techniques in mass production of LCDs consists in unidirectionally rubbing of the AL with textile materials. The orientation of LC molecules on such patterned surfaces is determined by PI chemical structure and conformation [14], rubbing parameters (rubbing force and density) [15], annealing [16], soaking solvent [17], and surface wetting characteristics [18]. Recently, it is shown that the type of rubbing textile fibers influences the polymer surface topography [19]. However, the alignment mechanism of LC molecules in contact with a rubbed polyimide surface is not entirely clarified. It is accepted that LC alignment results from the orientation of polymer chains in the outmost layer of the polyimide film due to rubbing [20].

Having all these in view, the present work is focused on investigation of some PIs based on naphthalene-containing dianhydrides and aromatic diamines with oxadiazole rings. The effect of chemical structure on the resulting rheological functions is evaluated in order to determine the optimal processing conditions of the solutions into films. The morphology of these poly(oxadiazole-imide)s is designed through rubbing with two types of velvet. The resulted morphological features are discussed in correlation with both chemical structure and patterning conditions. Preliminary testing of the orientation ability of these processed PI films is performed using a nematic LC, such as 4′-pentyl-4-biphenylcarbonitrile (5CB).

Experimental

Synthesis of polymers

The chemical structures of investigated PIs containing oxadiazole units and naphthalene rings are presented in Scheme 1. The detailed synthesis of these polymers and their basic characterization is described elsewhere [21–23]. In brief, poly(oxadiazole-naphthylimide)s, PI1–PI4, are prepared by polycondensation reaction in solution at high temperature (200 °C) of an equimolar amounts of aromatic oxadiazole-diamines with a mixture of hexafluoroisopropylidene-diphthalic dianhydride and bis(ketonaphthalic-anhydride) or naphthalene-1,4,5,8-tetracarboxylic acid dianhydride, taken in different molar ratios. The polycondensation reaction is carried out in *N*-methylpyrrolidinone (NMP), in the presence of benzoic acid as catalyst, at a concentration of 10–12 % total solids. The monomer ratio is adjusted up to soluble, and film-forming polymers are obtained. The resulting PI solutions in NMP are used partly to cast thin films and partly to isolate the solid polymer by precipitation into water. All PIs are soluble in NMP and their solutions are stable, when stored for long time (6 months) at room temperature.

Preparation of polymer solutions

A standard procedure for preparing the sample solutions is used. First, the PI powder is weighed and put into a jar (also weighed). The polymer is then mixed with an appropriate amount of NMP to obtain the following concentrations: 2, 4, 6, 8, 10, and 12 % for each polymer. The jar was tightly sealed and gently stirred for assuring the homogeneity of the solution.

Preparation of polymer films

Films of poly(oxadiazole-naphthylimide)s, PI1–PI4, are prepared by casting a filtrated solution of 10–12 % concentration of polymers in NMP onto glass plates, followed by gradual heating from room temperature up to 210 °C, and kept at 210 °C for 1 h. Transparent coatings resulted having strong adhesion to the glass support. The resulting films are stripped off the plates by immersion in water followed by drying in oven at 100 °C. These films have the thickness of approx. 40 μm and are subjected afterward to patterning and testing the alignment ability of a nematic

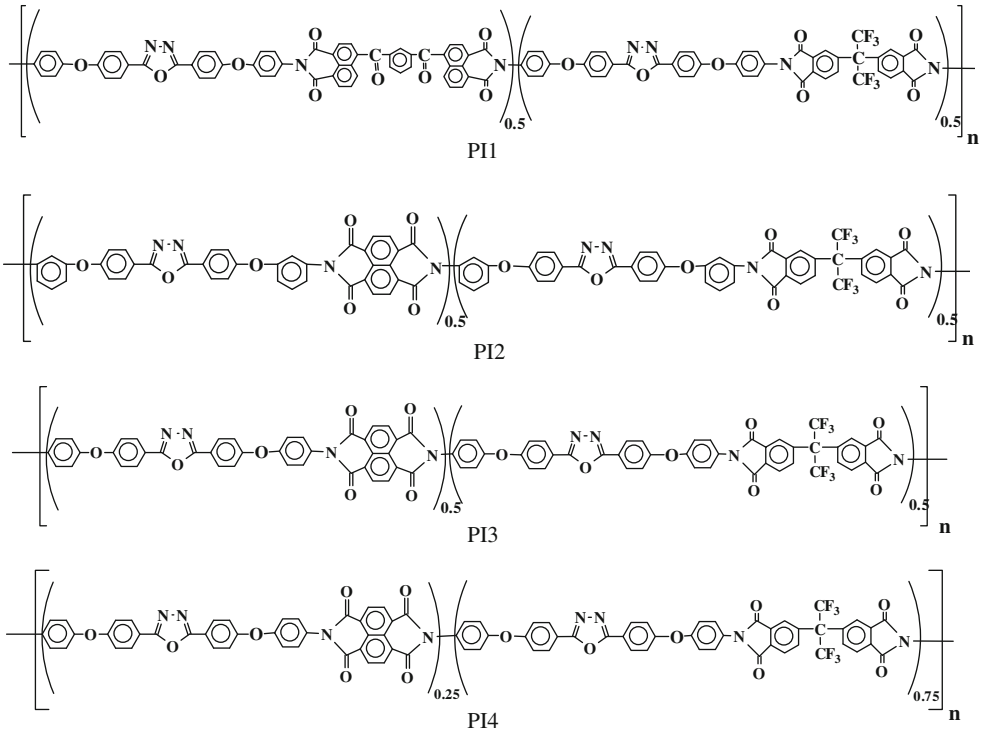

Scheme 1 Chemical structures of investigated poly(naphthylimide)s containing oxadiazole rings

LC, namely 4′-pentyl-4-biphenylcarbonitrile (5CB, Sigma Aldrich).

Measurements

Average-molecular weights of the polymers are measured by means of gel permeation chromatography (GPC) using a Waters GPC apparatus, provided with Refraction and UV Photodiode array detectors and Shodex column. Measurements are carried out with polymer solutions having 2 % concentration, and using DMF/0.1 mol $NaNO_3$ as solvent and eluent, with a rate of 0.6 mL/min. Polystyrene standards of known molecular weight in solution of DMF/0.1 mol $NaNO_3$ are used for calibration.

The infrared spectra of the polymers are recorded on FT-IR Bruker Vertex 70 Spectrophotometer in reflexion mode, using free-standing thin films.

Optical transparency of the films is recorded at 300–1100 nm wavelengths, on a SPECORD 200 Analitik-Jena spectrophotometer.

The flow properties of the PI solutions are determined on a Bohlin CS50 rheometer, manufactured by Malvern Instruments. The measuring system presents cone-plate geometry with a cone angle of 4° and a diameter of 40 mm. Shear viscosities are registered over the 0.1–1000 s^{-1} shear rate domain for recording all possible flow regimes. During the oscillatory shear tests, the frequency is ranged between 0.01 and 15 Hz, and a shear stress of 2 Pa is selected from the linear viscoelastic domain, where the rheological moduli are independent of the shear stress.

Mechanical properties of the polymer films are analyzed by tensile testing using an Instron 5566 apparatus. The samples are used in the form of strips having the thickness of 0.04 mm, gage length of 25 mm and width of 15 mm. Stiffness, tensile strength, and elongation-at-break are determined at 10 mm/min cross-head speed. The dependencies of tensile stress (MPa) versus tensile strain (%) are recorded.

Surface rubbing is performed using an instrument constructed in our laboratory based on a rotating cylinder of 12 mm diameter, which is covered with velvet. The rotation speed is maintained constant (200 rot/min) along with the rubbing pressure. The poly(oxadiazole-naphthylimide)s films are processed during 1 min, using two types of velvet: a natural one from cotton (V_C), and a synthetic one made from cellulose diacetate (V_{CD}). A liquid crystal cell is constructed in order to verify if the rubbed polyimide surfaces are able to produce the orientation of 5CB. This nematic compound exhibits liquid crystal phase near room temperature and its refractive index is of 1.53. The LC cell consists of two rubbed polyimide films, separated by a uniform gap (of 5 μm) in which the nematic LC is introduced with a microsyringe. The cell is examined under an optical microscope between crossed polarizers. The experiment involves studying the

5CB alignment by rotating the sample 360° to observe the changes in light intensity.

The texture of the rubbing textile fibers is investigated on an Environmental Scanning Electron Microscope (ESEM) type Quanta 200.

Polarized light microscopy (PLM) investigations are performed on an Olympus BH-2 polarized light microscope.

In order to investigate the surface morphology changes induced by rubbing process, the samples are analyzed by atomic force microscopy (AFM) technique, using a Solver Pro-M Scanning Probe Microscope (NT-MDT, Russia). Rectangular silicon cantilevers NSG10 (NT-MDT, Russia) with resonance frequency of 288 kHz and tips of high aspect ratio are used. All images are acquired in air, at room temperature (23 °C), in semi-contact mode, with a scanning frequency of 1.2 Hz. The scan lengths are 2 μm for the pristine polymer films; and 5 μm for the rubbed polymer films. These scan lengths are chosen so that the morphological features to be more easily observed. For image acquisition and processing Nova v.1.26.0.1443 for Solver software is used.

Results and discussion

Structural characterization of the polyimide films

The structures of the polyimide films are identified by means of IR spectroscopy. In the FTIR spectra the sharp band at 3480–3490 cm^{-1} is assigned to the N–H stretching vibration of polymer chain, to the end NH_2 groups or to NH groups in polyamidic acid incompletely imidized during polymer synthesis. The broad absorption at 3070–3080 cm^{-1} belongs to the C–H stretching vibrations of the aromatic rings. The characteristic five-member imide ring absorptions appeared at 1780–1790 cm^{-1} (asymmetrical C=O imide stretching) and 1720–1740 cm^{-1} (symmetrical C=O imide stretching), while the six-member imide structure gave absorptions at 1720–1740 cm^{-1} (superposed on five-imide ring absorption) and 1670–1680 cm^{-1}. The sharp peaks at 1590–1600 and 1480–1490 cm^{-1} are assigned to the stretching vibrations of aromatic systems, i.e., the 1,4-disubstituted phenylene rings. The broad absorption at 1370–1375 cm^{-1} is assigned to C–N stretching in imide ring, while the band at 1240–1250 cm^{-1} is ascribed to asymmetric C_{Ar}–O–C_{Ar} stretching vibration of diaryl ether group. Characteristic absorption peaks of 1,3,4-oxadiazole ring are identified at 1012–1024 cm^{-1} and 970–983 cm^{-1} (=C–O–C= stretching). The sharp band at 720–731 cm^{-1} corresponds to the out-of-plane bending vibration of the imide ring. Figure 1 shows a representative FTIR spectrum for these polyimides.

The molecular weight values of the polyimides PI1–PI4 were measured by gel permeation chromatography (GPC), using polystyrene standards. The molecular weight values, Mw, are in the range of 41500–115500 Da, Mn in the range of 23400–63300 Da, and polydispersity (PI) Mw/Mn in the range of 1.73–1.82. As can be seen in Table 1, the present polymers have fairly high values of molecular weight and very narrow molecular weight distribution.

Rheological analysis of solution microstructure

Since, processing of polyimide ALs almost always implies a liquid–solid transition, the effect of some external factors on rheological functions, related to the resulting film properties, is investigated.

Viscosity is one of the most important rheological parameters in solution processing, which depends on the molecular structure, the molecular weight distribution, and chain interactions [24]. The latter are influenced by the rigidity, symmetry, and regularity of the molecular backbone. Molecular entanglements affect zero shear viscosity and subsequent strength of the processed film. In order to identify the different concentration regimes in which polymer chain entanglements dominate the flow behavior, the solution rheological properties of the poly(oxadiazole-naphthylimide)s are investigated on a wide concentration range. The dilute concentration regime, where the polymer chains are distributed randomly as separate spheres, is not studied since in this domain no interchain entanglements occur. In this case, separated chains behave more or less independently, the polymer molecules mainly interacting with the solvent molecules [25]. In the semidilute range it is reported that specific viscosity dependence on concentration exhibits two different power law dependences [26, 27]. For neutral linear polymers in a good solvent, specific viscosity $\eta_{sp} \sim c^{1.25}$ in semidilute unentangled regime and $\eta_{sp} \sim c^{4.25–4.5}$ in semidilute entangled domain [28].

In order to calculate specific viscosity, $\eta_{sp} = (\eta_0 - \eta_{NMP})/\eta_{NMP}$, the zero shear viscosities, η_0, are approximated from the flow curves using the actual or extrapolated values for apparent viscosity at 0.1 s^{-1}. The η_{sp} as a function of concentration for the poly(oxadiazole-naphthylimide)s solutions in NMP is plotted in Fig. 2. It can be noticed that at low concentration the slope of η_{sp} is varying between 1.1 and 1.3. This is indicative of the onset of the semidilute unentangled domain, where the concentration is large enough to produce few chains overlap. As the concentration is further increased, the topological constraints induced by the larger occupied fraction of the available hydrodynamic volume in solution introduce chain entanglements. The change in the slope of $\eta_{sp} \sim c^{3.4–4.8}$ marks the semidilute entangled regime. The crossover of the linear regressions corresponding to the semidilute unentangled and semidilute entangled regimes defines the critical entanglement concentration, c_e.

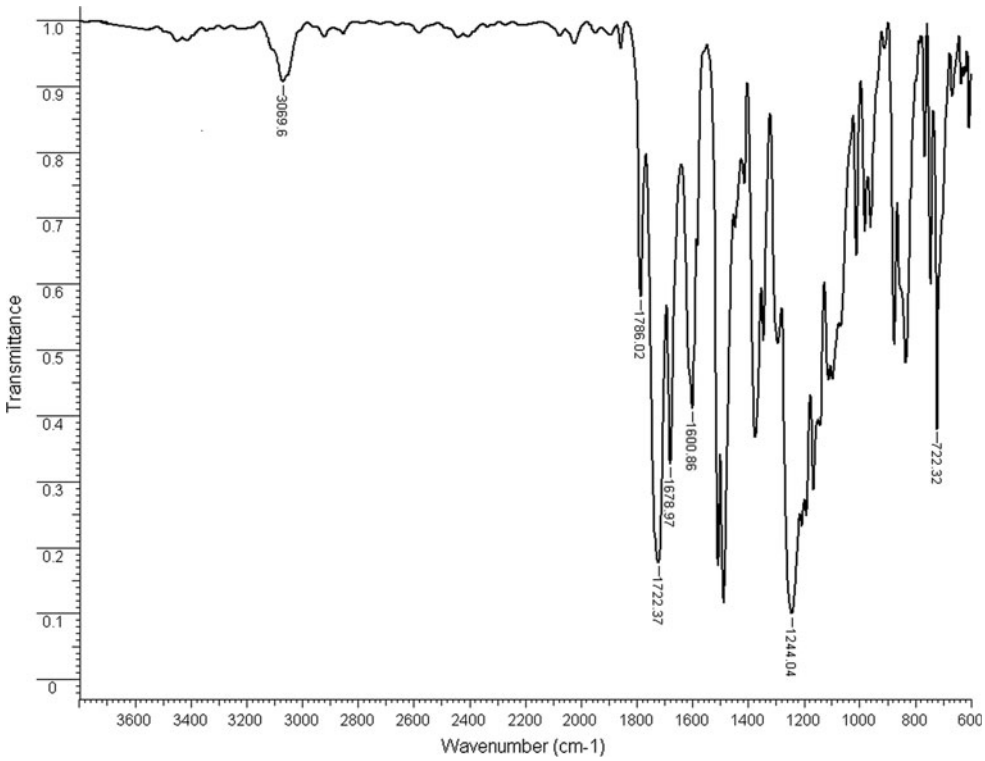

Fig. 1 FTIR spectrum of the polyimide PI4

Table 1 The values of Mw, Mn, and polydispersity index (PI) for the poly(oxadiazole-naphthylimide) samples

Polymer	Mw (Dalton)	Mn (Dalton)	PI
PI1	115500	63300	1.82
PI2	98700	55500	1.78
PI3	41500	23400	1.77
PI4	50200	29100	1.73

This parameter is dependent on the PI molecular weight and chain conformation.

For instance, in the case of PI1, which has the highest M_n, the entanglement of the macromolecular chains occurs earlier comparatively with the other samples. This is supported by the values of c_e which are increasing with the decreasing of M_n, as depicted in Fig. 2. The polyimide with the lowest molecular weight and the most rigid structure, PI3, requires a higher critical concentration (7.11 %) for the entanglement of the chains, compared with the other polymers. Below c_e the solution viscosity is controlled by the intramolecular excluded-volume effects, whereas above c_e the intermolecular entanglements have a prevalent effect on the rheology of the solution [26].

The influence of these aspects is reflected in the flow behavior, described by shear viscosity. Its dependence on shear rate for the studied poly(oxadiazole-naphthylimide) solutions in NMP at 25 °C is plotted in Fig. 3. At low concentrations PI1 and PI2 exhibit a shear-thinning domain, followed by a constant viscosity region, appearing at shear rates higher than approx. 10^2 s^{-1}. The resulted behavior is in agreement with literature data [29] which show a non-Newtonian flow for some conventional aromatic PI solutions below 3×10^{-2} s^{-1}, by means of the cone and plate measuring system. Conversely, PI3 and PI4 at 0.1–1 s^{-1} present a Newtonian plateau, subsequently continued with a pseudoplastic behavior. At high concentrations (>8 %) the flow behavior is prevalently Newtonian, excepting PI3 and PI4, for which the viscosity slightly decreases at high shearing since the flexible 4,4′-(hexafluoroisopropylidene)-diphthalic anhydride (6FDA) moieties and *p*-substituted ether linkages suffer an orientation process. The different flow behavior of the samples can be explained by considering the backbone flexibility and molecular weight. The poly(oxadiazole-naphthylimide)s PI1 and PI2 exhibit higher M_n comparatively with PI3 and PI4, therefore, they are more difficult to orient during shearing. Also, higher rigidity of PI2 determines a lower packing efficiency and after subjecting it to the shear field fewer chains are unentangled conducting to a smaller slope of the thinning region, while for PI1 the viscosity decreases faster because of its flexibility allows better mobility under shearing. When comparing the other two samples it can be noticed that there is a synergism between the higher flexibility of PI4, given by the presence of more 6FDA sequences, and its higher M_n.

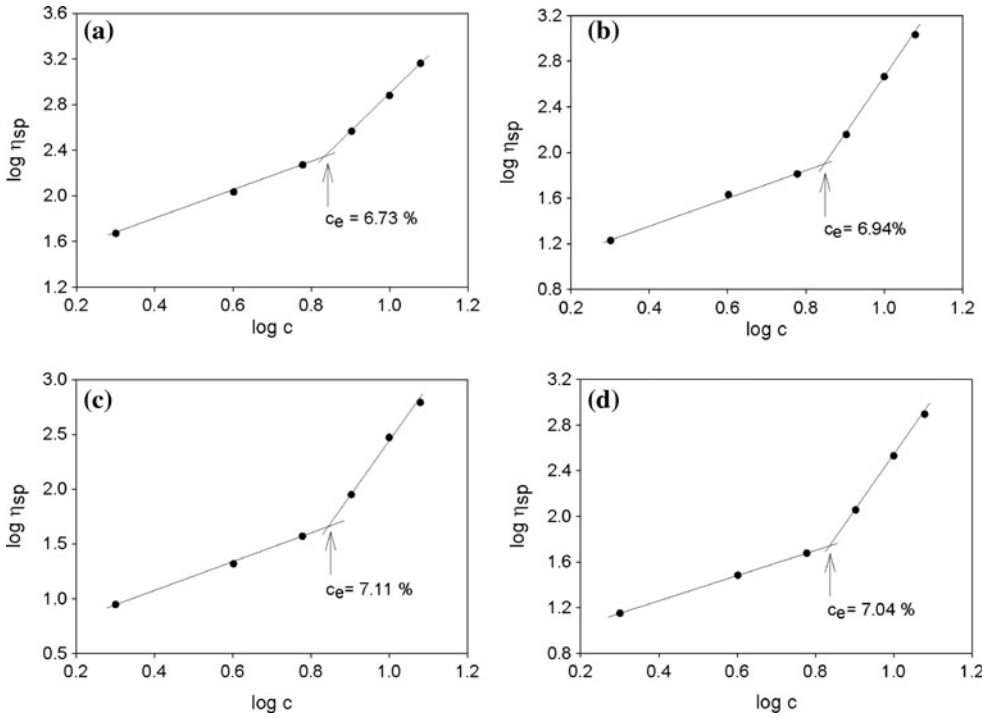

Fig. 2 Specific viscosity dependence on concentration for **a** PI1, **b** PI2, **c** PI3, and **d** PI4

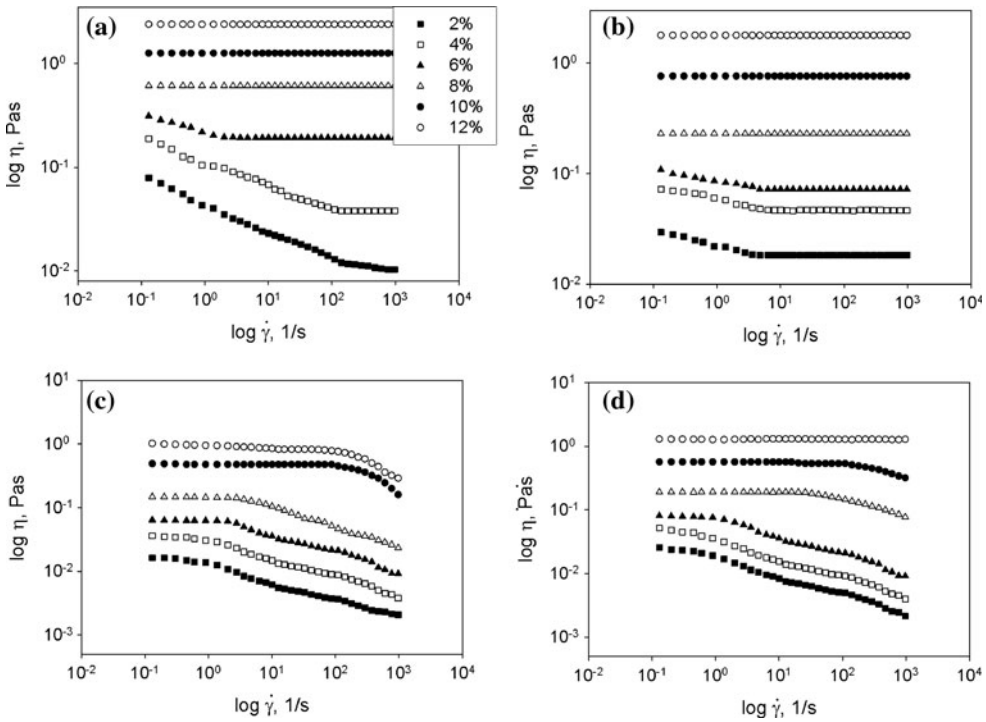

Fig. 3 Shear viscosity dependence on shear rate for **a** PI1, **b** PI2, **c** PI3, and **d** PI4 at room temperature

When processing the polyimide solution by shear casting or spin coating, the variation of viscosity under a deformation force is very important. The film thickness and uniformity represent critical factors influencing the morphology and properties of polymers and the performance of devices in which they are implemented. The literature survey [30] on this matter shows that the thickness profiles of a non-Newtonian fluid leads to nonuniform dried films. Thus, shear-thinning fluids produce films that are uniform near the axis of rotation, thus the thickness decreases away from the axis of rotation. Conversely, the initial thickness profile of a Newtonian solution tends to smooth out with spinning time

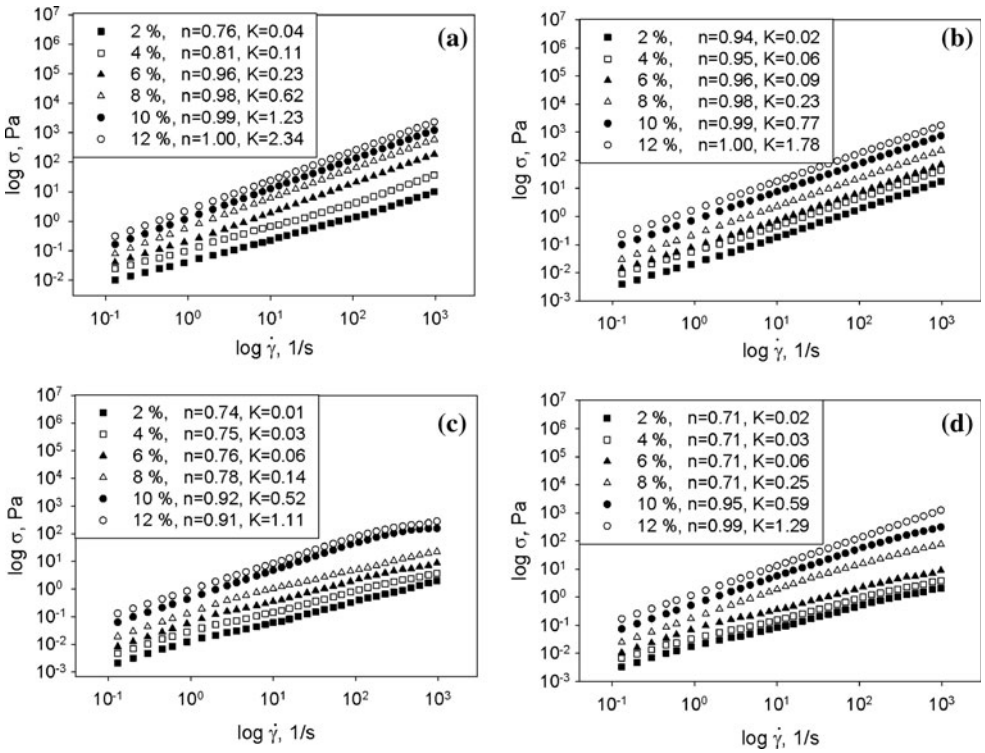

Fig. 4 Shear stress dependence on shear rate for **a** PI1, **b** PI2, **c** PI3, and **d** PI4

leading to uniform films. Simple modeling revealed that spinning at lower rates results in a more uniform coating [30]. For obtaining proper films from poly(oxadiazole-naphthylimide) solutions, here under analysis, it is better to use concentrations above c_e, and the samples should be shear casted/spin coated at shear rate/rotation velocity selected from the domain in which the viscosity is Newtonian.

The variation of shear stress, σ, with shear rate, $\dot{\gamma}$, for all concentrations taken into study, is presented in Fig. 4. This dependence obeys the power law relationship expressed as:

$$\sigma = K \cdot \dot{\gamma}^n \tag{1}$$

where n and K are the flow behavior and consistency indices, respectively.

Literature [31–33] shows that for a Newtonian fluid the flow behavior index is equal to the unity, while for a thinning liquid is lower than unity. For all samples, the shape of curves representing log shear stress versus log shear rate plots is different, as observed from Fig. 4, where two flow regimes are distinguished. Therefore, the flow curves exhibit two regions characterized by different slopes. At low concentrations the power law index, n, is less than one revealing a shear-thinning (pseudoplastic) behavior. After 8 % the shear stress of all samples becomes linear, having the slope of approx. 1, highlighting the Newtonian behavior. The resulted values of flow behavior and consistency indices of the studied PI solutions determined from the linear regression corresponding to flow curves are listed in Fig. 4. It can be observed that the flow consistency index increases with increasing concentration. Also, any increase in concentration is accompanied by a decrease in pseudoplasticity, shown by the increase in the values of the flow behavior index. The consistency index can also be correlated with the molecular weight of the investigated polyimide solutions. Thus, the sample PI1 of highest M_n presents higher consistency index comparatively with the other ones.

The analysis of the correlation between the flow behavior and the structural characteristics is essential for obtaining resistant and dimensionally stable polymer films implemented in electronic devices. In addition, the viscoelastic characteristics are determining the quality of the polyimide films. The rheological parameters describing these properties are the elastic (storage) modulus, G', the viscous (loss) modulus, G''. The first one represents the strain energy reversibility stored in the sample, and it depends on the number and strength of the interactions from the system. The liquid-like response is denoted by the G'', which gives information on the unrecoverable viscous loss. The variation of the viscoelastic moduli with frequency (f) is shown in Fig. 5 for investigated solutions of 12 %, at 25 °C. In order to insure the fact that oscillatory shear measurements are maintained in the linear viscoelastic domain, a fixed shear stress of 1 Pa is selected. At low frequencies the sample response is described by a frequency power law of shear moduli, i.e., G' and G'' are proportional to approx. f^2 and f^1, respectively. In this region

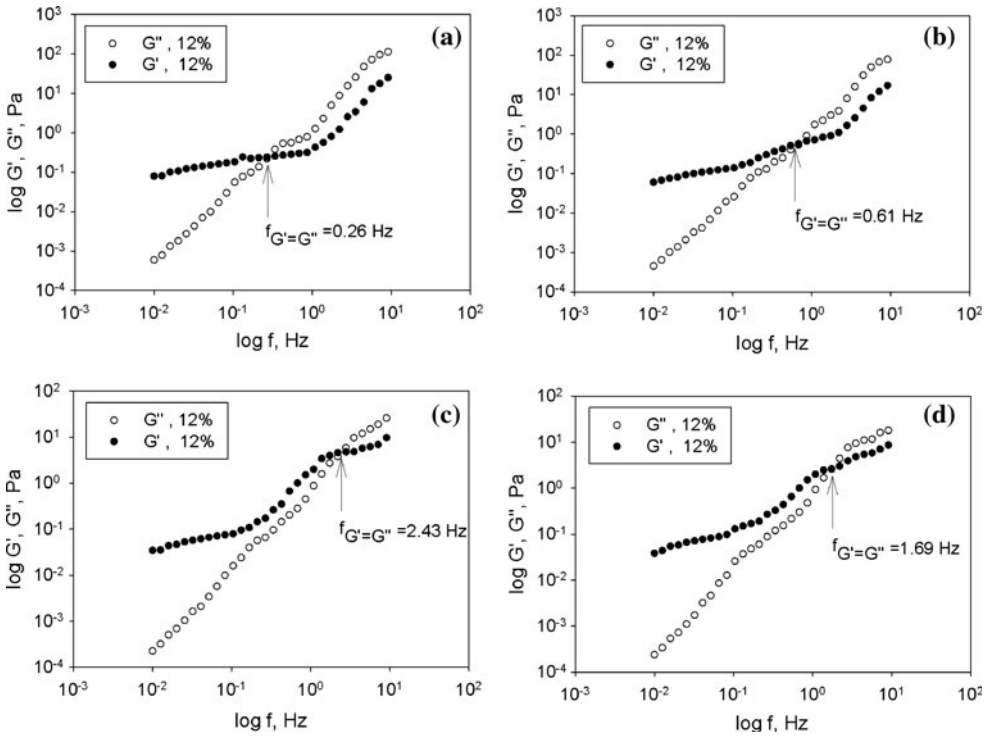

Fig. 5 Shear moduli dependence on frequency for **a** PI1, **b** PI2, **c** PI3, and **d** PI4

G'' is always higher than G' [34], whereas at higher frequencies, G' becomes higher than G''. In other words, at low frequencies the liquid-like behavior prevails as a result of unrecoverable viscous loss, while at high frequencies the solid-like character becomes predominant and determines energy reversibility stored in the sample, as a result of the number and strength of interactions from the system. At the highest studied concentration (12 %) the dominant elastic response is seen in a small rubbery region, where the storage modulus shows a plateau. It is well known that the plateau region appears for polymers with entanglements in solution and is more clear and pronounced in higher molecular weight polymers, as shown in Fig. 5 [35].

The crossover frequency ($f_{G'=G''}$) of shear moduli increases with the decreasing molecular weight. The values of the overlap point are inversely proportional with the relaxation time. This parameter is a measure of the rate at which the global structure changes in response to the change in flow. During shearing the degree of anisotropy ranges with the speed and time duration of the flow. When returning to the quiescent state (no flow), the polymer solution relaxes to the original global isotropic condition. The force of reorientation to the isotropic condition of rigid microstructural units is caused by Brownian motion, while shape recovery of flexible microstructural elements is aided by internal springs. For the studied solutions, the relaxation time can be evaluated from the crossover frequency showed in Fig. 5. Modification of the chain interactions in solution are reflected in the values of crossover point, which delimits the viscous flow from the elastic flow. At high concentrations the enhancement of chain interactions decreases the free volume leading to the limitation of the chain motions at large scale. This involves high values of relaxation time, being indicative of prevalently elastic character of the PI solution. Therefore, the formation of chain entanglements prevents the dissipation of energy and preserves mechanical properties in solution optimum for preparation of resistant PI films, as required for ALs.

On the other hand, the differences in the viscoelastic behavior of the samples can be better analyzed with Cole–Cole plots. Such graphical representations are generally used in dielectric spectroscopy to investigate the changes in the polymer microstructure generated by the temperature [36]. Also, these plots can be used to elucidate structure differences at a fixed temperature [37]. For the polymers of interest, here the Cole–Cole plots are represented for 12 % solutions, according to Fig. 6. It can be noticed that when the storage modulus (for a given G'') is above the diagonal line the elastic character prevails in the following order: PI1 > PI2 > PI4 > PI3 (in agreement with the formation of molecular entanglements).

Considering the implications of chain flexibility and entanglement on flow behavior, the PI films are prepared from corresponding solutions in appropriate conditions as determined from their rheological properties. The obtained films are further tested to check if the solution properties are maintained in solid state.

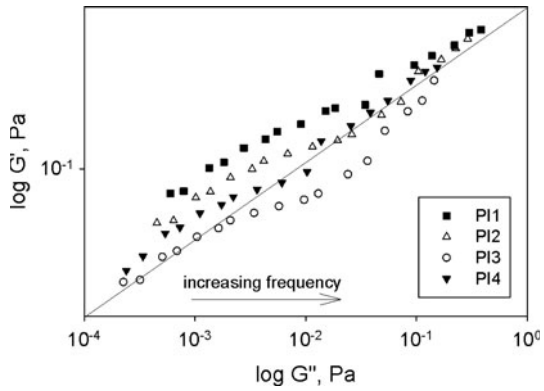

Fig. 6 Cole–Cole plots of elastic modulus versus viscous modulus for PI1–PI4 samples

Mechanical behavior

The polymer solutions (10–12 %) in NMP are processed into thin films by casting onto glass plates as described in the experimental part. The free-standing films having the thickness in the range of ~40 μm are flexible, tough, and maintained their integrity after repeated bending. The tensile properties of these polymer films are given in Table 2. Elastic modulus, tensile strength, and elongation to break have been determined as averages of three drawing experiments. The values of tensile strength are in the range of 31–113 MPa, elastic modulus in the range of 2.14–3.37 GPa, and elongation to break in the range of 1.88–7.51 %. These results are consistent with the rheological data. As can be seen in Table 2, the tensile properties of copolyimides PI1 and PI2, having higher molecular weights, are significantly higher than those of polyimides PI3 and PI4. At the same time, when comparing PI3 and PI4 with similar M_n, it can that a higher content of flexible hexafluoroisopropylidene (6F) groups in the repeating unit of copolyimide PI4 resulted in better tensile properties. Thus, judging from the point of view of mechanical behavior the molecular entanglements exhibit higher influence than chain flexibility. All these tensile data demonstrate that the films prepared from these poly(naphthylimide)s containing oxadiazole moiety and flexible 6F linkages are tough and can be used for further processing as LC orientation layers.

Table 2 Tensile properties of poly(oxadiazole-naphthylimide) films

Polymer	Tensile strength (MPa)	Elongation at break (%)	Modulus (GPa)
PI1	112.9 ± 2.69	6.2 ± 0.78	3.4 ± 0.08
PI2	100.6 ± 15.38	7.5 ± 0.84	2.6 ± 0.32
PI3	31.0 ± 1.65	1.9 ± 0.07	2.1 ± 0.40
PI4	69.9 ± 2.77	5.1 ± 0.37	2.3 ± 0.14

Optical properties

It is known that aromatic polyimide films, due to their high glass transition and decomposition temperature, low water absorption, good transmission, and low optical loss, are excellent candidates for use as transparent flexible substrates in displays or other electronic applications, especially active matrix type displays or organic thin-film transistors. All these provide that the formation of intra- and/or intermolecular charge-transfer complex (CTC) in the molecules is much reduced. Since the introduction of fluorine groups into the polyimide main chains is known to reduce the color and increase the transparency of the resulted films, the optical transmission of these fluorinated poly(oxadiazole-naphthylimide) films, PI1–PI4, by UV–Vis spectroscopy is analyzed. Figure 7 shows the optical transmission spectra of the polyimide films prepared as described in the "Experimental" section.

All the PIs revealed good optical transparency, with a percentage of transmittance up to 89 % in the wavelength range of 400–700 nm. As shown in Fig. 7, the optical transmission spectra of polyimide PI1, show the highest transparency in the visible region of this film, due to the presence of *meta*-catenated phenylene rings and hexafluoroisopropylidene groups that effectively reduced the intermolecular charge-transfer complex (CTC) formation between alternating electron-donor (diamine) and electron-acceptor (dianhydride) moieties. The kinking of phenylene rings which are connected in *meta* position to imide units significantly distorts the PI backbone and thus, the conformation of the main chain inhibits the conjugation of imide-phenyl bonds in the PI chains and reduces the intra- or intermolecular CT interactions. On the other hand the increase of fluorine content/structural unit of polyimide PI4 compared with PI3 is essentially for increasing its transparency being effective in reducing the CTC formation between polymer chains through steric hindrance, and the

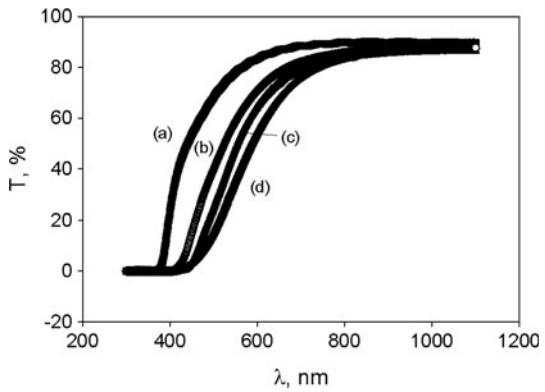

Fig. 7 Optical transmission spectra of (*a*) PI1, (*b*) PI2, (*c*) PI3, and (*d*) PI4 films

inductive effect and weakening chain-to-chain cohesive force due to lower polarizability of the C–F bond. Thus, it can be concluded that the studied polyimide films present good transparency in the visible domain, particularly PI1. These results show that the studied samples satisfy the requirement of transparency encountered for liquid crystal alignment layers.

Surface rubbing

In order to understand the effects created by the rubbing velvet fibers a comparative analysis between the pristine PI films and the patterned ones must be made. AFM measurements are employed for close examination of the samples morphological features. All four poly(oxadiazole-naphthylimide)s exhibit a relatively flat surface, randomly covered with nano-granules (Fig. 8). This type of topography is also observed for other PI films [19, 38]. The morphological aspect of these structural formations can be associated with the different packing ability of the studied polymers, due to some sequences existing in the macromolecular backbone, which induce a different flexibility for each copolymer. PI1 exhibits a higher packing ability owing to the flexible keto-naphthylimide and 6F moieties, as regards with PI2, and thus a lower peak-to-valley height. The same affirmation stands when comparing the PI4 with PI3, the former containing more rigid naphthylimide sequences. The balance between M_n values and differently substituted ether linkages lead to similar surface heights for PI2 and PI3.

Proper adaptation of the polyimide surface for obtaining an AL is made with two types of velvet: cotton velvet (V_C) and cellulose diacetate velvet (V_{CD}). Each fiber tip consists of subfibrous filaments that have a broad range of diameters, from a few submicrometers to a few micrometers. The subfibrous filaments at the fiber end might generate microroughness in the film surface by their contact with the polymer. The aspect, shape, and size of the constituent textile fibers used in this study are presented in Fig. 9. The ESEM images show that the length and thickness of V_C are 950 μm length and 15 μm, respectively, and that of V_{CD} are 1.5 mm and 25 μm, respectively. The rubbing process changes the initial isotropic surface into an anisotropic one. This can be noticed in the PLM images of the rubbed samples (Fig. 10).

At the nanometric level, AFM data reveal that for all films the granular formations disappear and some microgrooves lines are formed parallel to the rubbing direction. The difference regarding the AFM images from Figs. 11 and 12 consist in the used rubbing fabric. Figure 11 reveals the morphology of all PI1–PI4 films developed after rubbing with cotton velvet, while Fig. 12 shows the surface features after rubbing with cellulose diacetate velvet. The obtained results are important since they show that the type of rubbing velvet determines the grooves depth and surface uniformity. This aspect is significant in practical

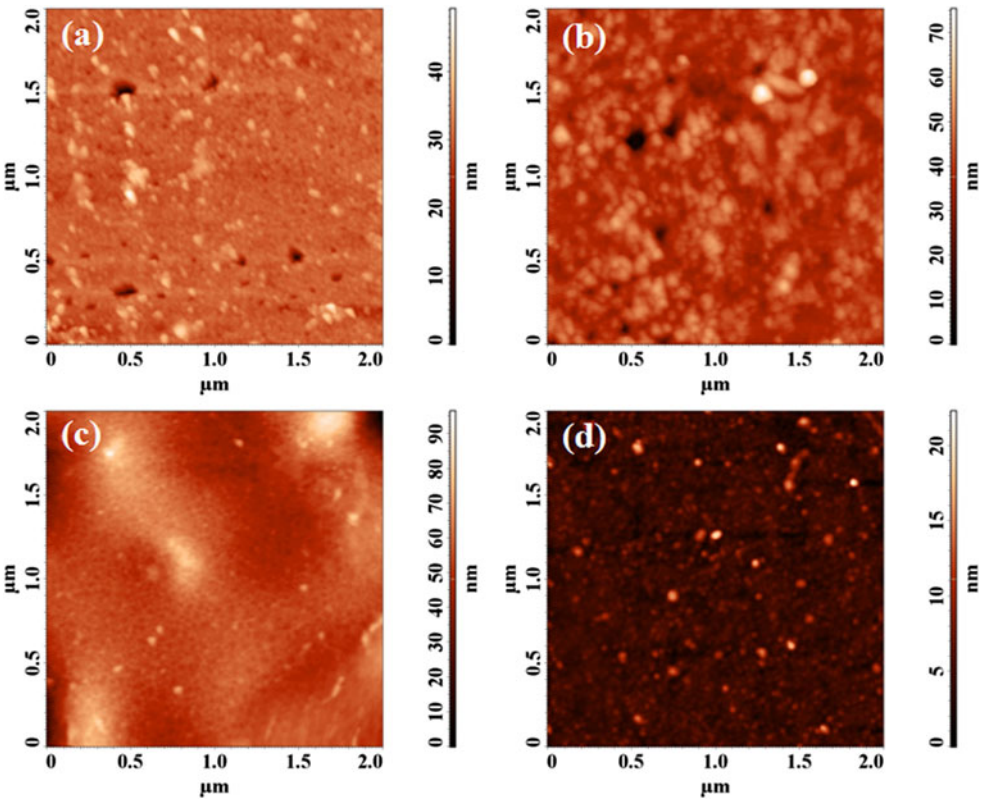

Fig. 8 AFM images for pristine polyimide films **a** PI1, **b** PI2, **c** PI3, and **d** PI4

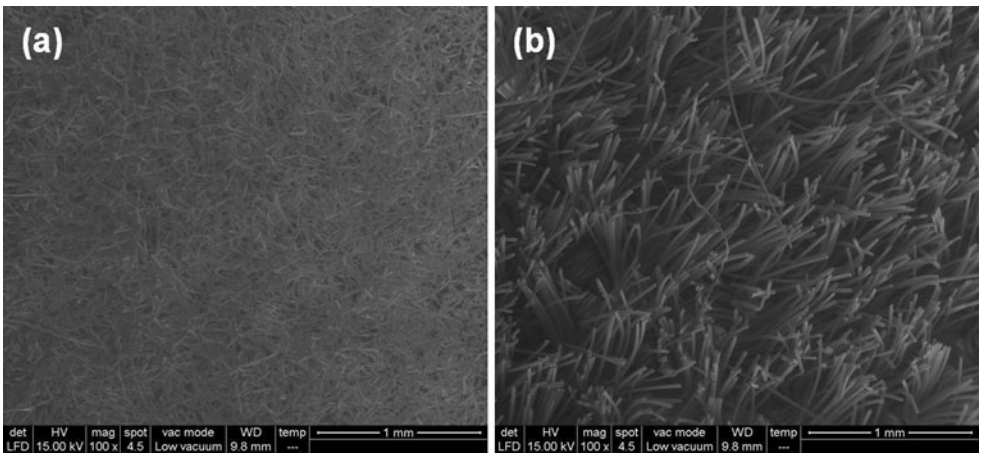

Fig. 9 ESEM images obtained for **a** cotton velvet and **b** velvet of cellulose diacetate

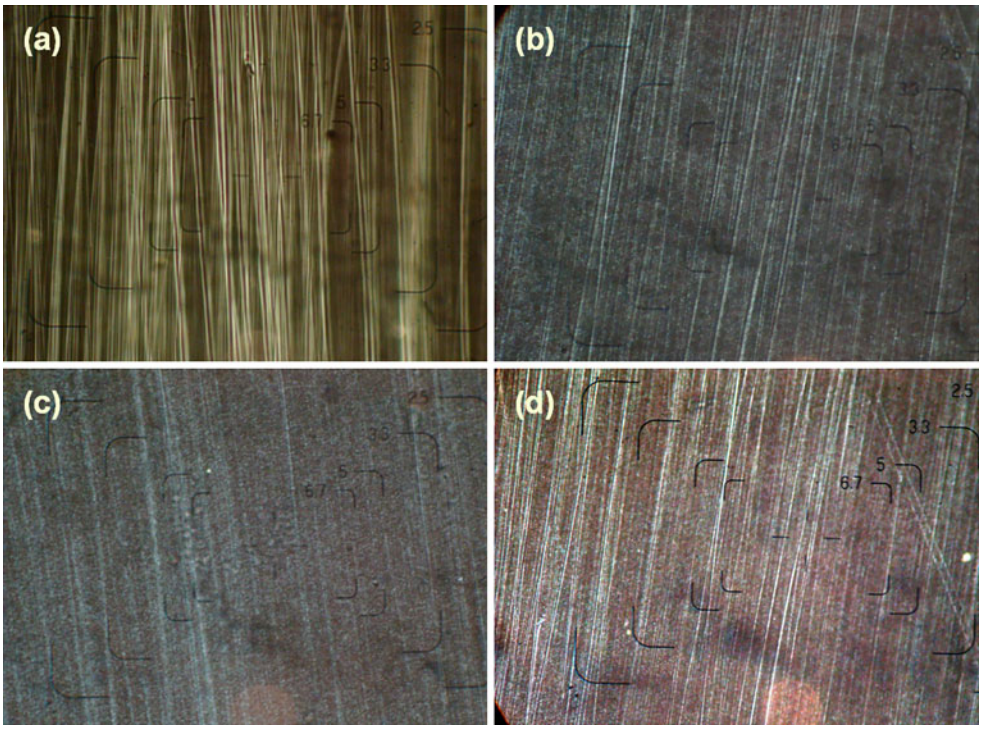

Fig. 10 PLM images obtained for **a** PI1, **b** PI2, **c** PI3, and **d** PI4 rubbed with cellulose diacetate. The polarizers are at 45° and the magnification is 200×

applications, since it influences the alignment of liquid crystals on the polyimide surface. According to surface topographic mechanism or elastic distortion model of Berreman [39], the developed morphology is known to be essential for the alignment of LC molecules. The detailed modifications created in polyimide surface by rubbing with V_C and V_{CD} are observed in bidimensional AFM images and their corresponding section profiles.

The first aspect that must be taken into consideration when discussing the developed morphology is the deformation response of the PI to the shear force produced by the fibers during rubbing. At constant rubbing density or the rubbing pressure, the molecular reorientation occurs deeper within the polyimide surface layers. Supplementary or more intense rubbing do not further influence the chain orientation. Regardless of the rubbing fabric, it can be observed that the penetration depth of the rubbing process depends on the degree of entanglements. As the molecular weight is higher (more entanglements) the depth of resulted microgrooves is smaller. Thus, according to the section profiles from

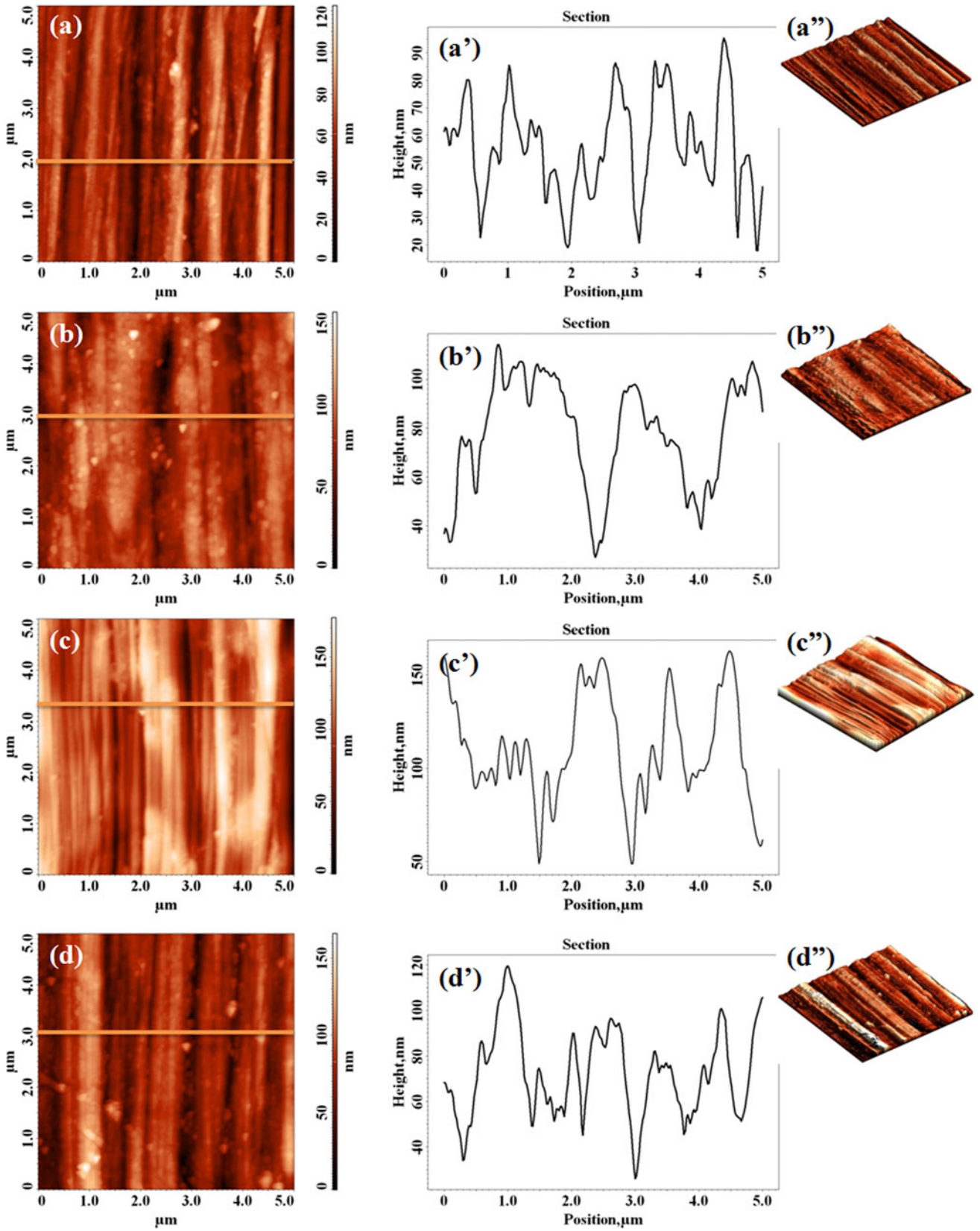

Fig. 11 AFM images, cross-section profiles, and 3D images for (**a**, **a′**, **a″**) PI1, (**b**, **b′**, **b″**) PI2, (**c**, **c′**, **c″**) PI3 and (**d**, **d′**, **d″**) PI4, respectively, after rubbing with cotton velvet

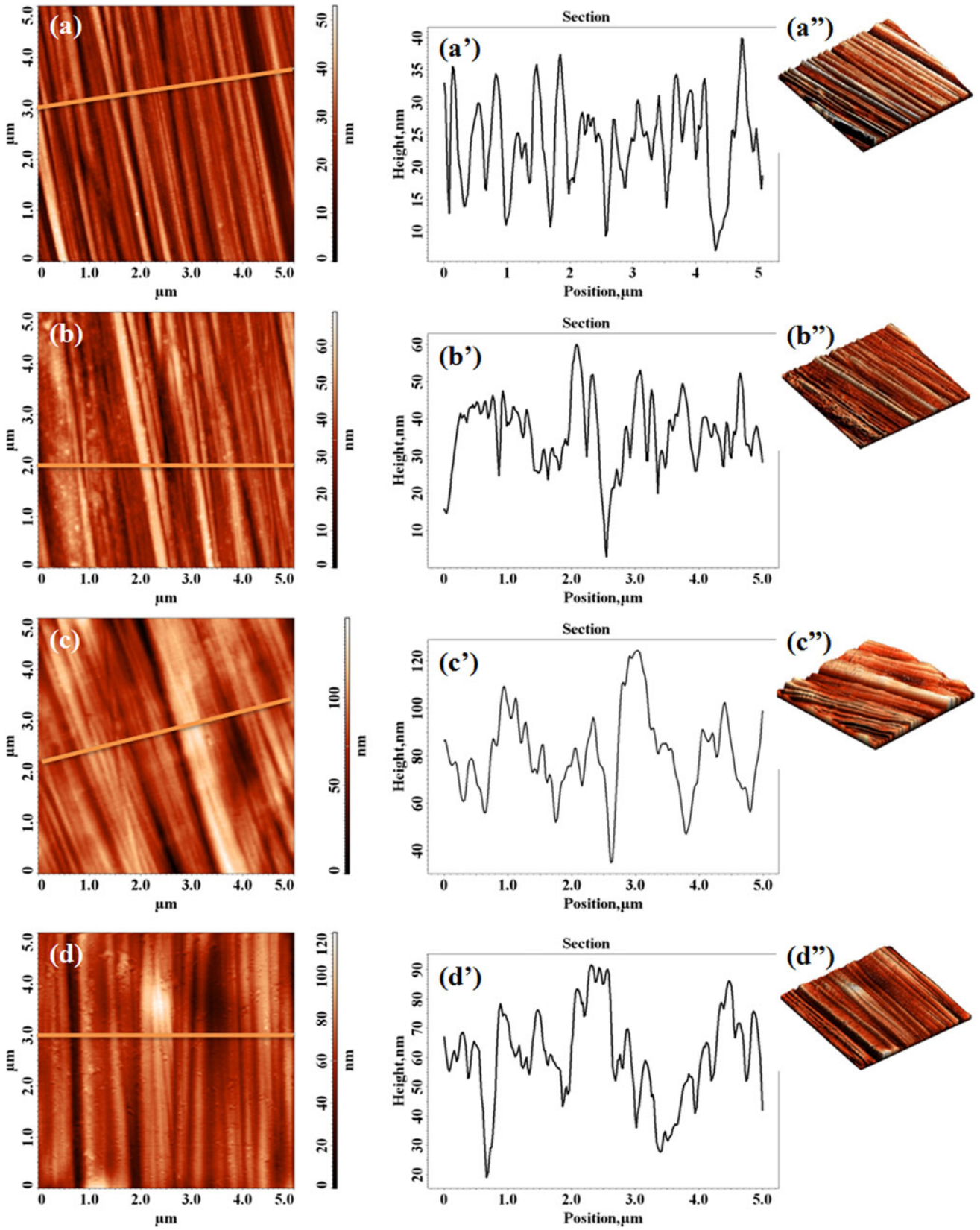

Fig. 12 AFM images, cross-section profiles, and 3D images for (**a**, **a′**, **a″**) PI1, (**b**, **b′**, **b″**) PI2, (**c**, **c′**, **c″**) PI3 and (**d**, **d′**, **d″**) PI4, respectively, after rubbing with cellulose diacetate velvet

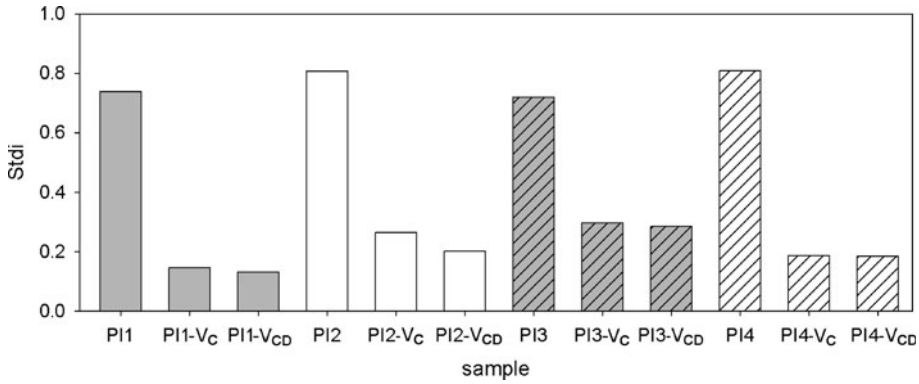

Fig. 13 The values of Stdi parameter for each studied sample

Figs. 11a′–d′ and 12a′–d′, PI1 sample presents shallower microgrooves, comparatively to the other studied PIs. Literature [40] shows that the aligning of LC is mainly determined by the chain reorientation at polyimide film surface and secondly by microgrooves, suggesting that molecular-level interactions between LC and polyimide prevail in regard with the mechanical interactions. The introduction of flexible sequences into PI backbone is useful for increasing the interactions between the flexible parts of the PI and LC molecules, since it enhances pretilt angles [41]. Therefore, the PI film surface uniformity and regularity are of extreme importance for LCD reliability. The degree of PI surface orientation is analyzed through surface texture direction index (Stdi). This parameter is the measure of how dominant the prevailing direction is, and is defined as the average amplitude sum divided by the amplitude sum of the dominating direction. Surfaces with very dominant directions will have Stdi values close to zero, while surfaces with the amplitude sum similar for all directions have Stdi near unity. The pristine PI films exhibit Stdi values close to 1, ranging from 0.720 to 0.808 (Fig. 13). Rubbing process determines a decrease of Stdi below 0.5 as a result of the generated surface anisotropy. Comparing the two fabrics it can be noticed that V_C leads to slightly higher Stdi, comparatively with V_{CD}, revealing that this material induces a weaker orientation of PI chains. The differences in the surface reorganization and pattern uniformity of studied samples can be explained by considering the competitive effects of the entanglements and PI backbone flexibility, which dictate the shear-induced deformation response and implicitly the magnitude of Stdi parameter. For instance, it is expected that a more flexible structure may be more easily to orient during rubbing, but at the same time the degree of entanglements, which assures a uniform response to the applied force, limits the chain mobility. Considering the order in which the Stdi data range, it can be concluded that a minimum degree of entanglements is required for insuring the surface uniformity, but the dominant factor determining the chain orientation is the backbone flexibility (PI1 > PI4 > PI2 > PI3).

The shape of the surface height distribution (revealed in Fig. 14) was another important component of the pristine and rubbed poly(oxadiazole-naphthylimide) films surfaces that was examined by means of two 3D topographic parameters, such as surface skewness (Ssk) and coefficient of kurtosis (Sku), which measure the departure from a Gaussian distribution of surface heights, but emphasize different aspects of departure from normality. In order to monitor the morphology development induced by the rubbing process, the evaluation of the Ssk, representing the degree of symmetry of the surface heights reported to the mean plane, was very useful. Generally, Ssk is sensitive to occasional deep valleys or high peaks, since it depends on whether the surface dislevelment is above (negative skewed) or below (positive skewed) the mean surface height. As observed from Table 3, the Ssk values of pristine surfaces were positive. These showed that all four samples reveal profiles with valleys filled in and occasional high peaks. On the other hand, the negative skewness obtained for the rubbed samples indicates the preponderance of valley structures comprising the surface. The investigation of the Sku parameter was meaningful in indicating the presence of either peak or valley defects, which may occur on a surface. Analyzing the higher positive values of the coefficient of kurtosis obtained for the unmodified copolyimide films presented in Table 3, it can be suggested that the surfaces have relatively little area high above or below the mean plane. Also, this implies that these surfaces have leptokurtic peaks, since Sku > 3. Moreover, the lower values of the kurtosis (Sku < 3) obtained for the rubbed poly(oxadiazole-naphthylimide) films with bumpy morphology, indicate that the surfaces have a relatively even distribution of heights above and below the mean height, these surfaces being called platykurtic. Measurement of this additional parameter brings further evidence that the rubbing process induce surface reorganization and pattern uniformity.

However, the size and the mechanical properties of the textile fibers can not be neglected because they are further

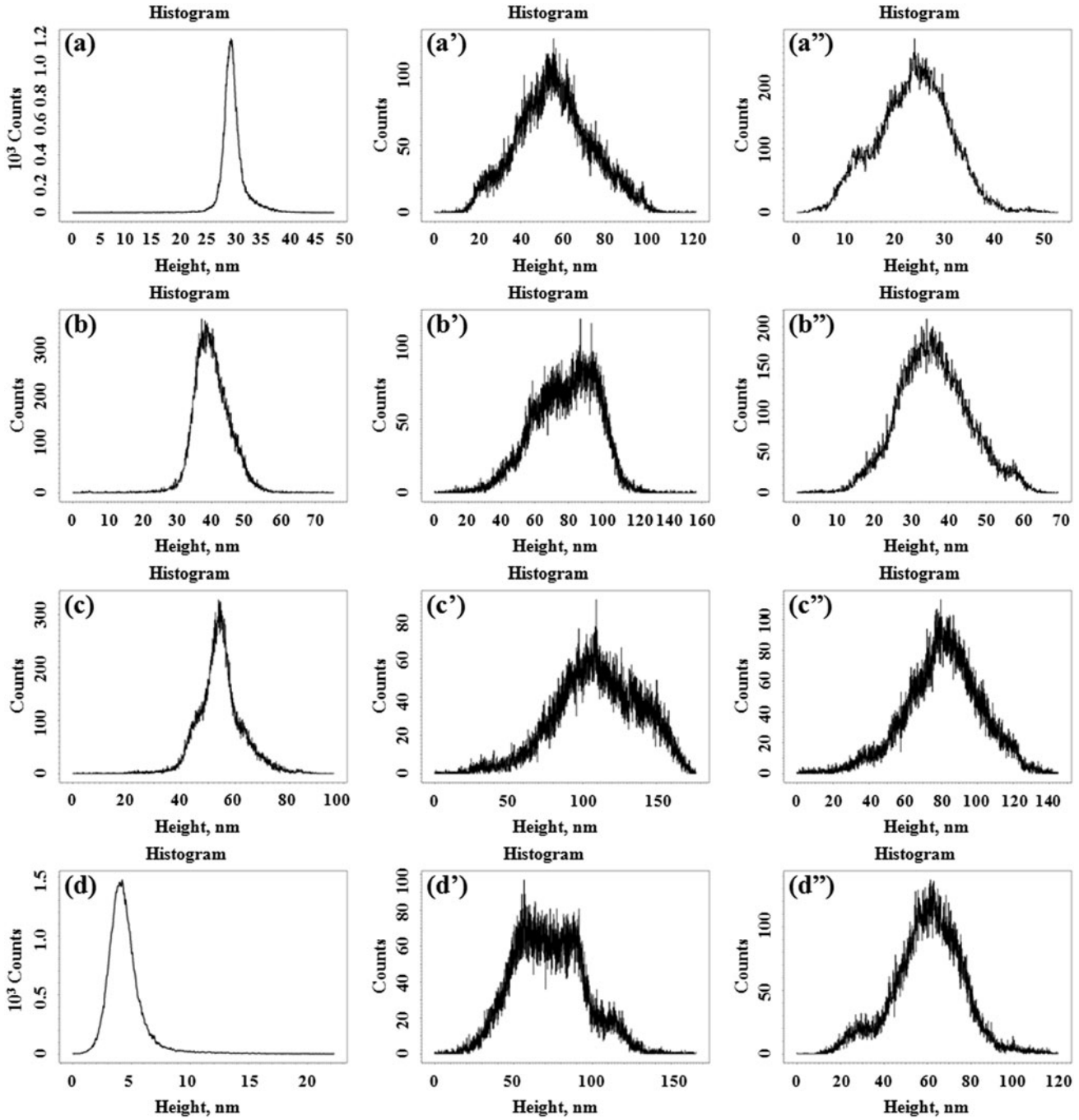

Fig. 14 Height histograms used for surface texture parameters determination (Ssk and Sku) for (**a**) PI1, (**a′**) PI1–V_C, (**a″**) PI1–V_{CD}, (**b**) PI2, (**b′**) PI2–V_C, (**b″**) PI2–V_{CD}, (**c**) PI3, (**c′**) PI3–V_C, (**c″**) PI3–V_{CD}, (**d**) PI4, (**d′**) PI4–V_C, and (**d″**) PI4–V_{CD}

determining the surface features. The cellulose diacetate is constituted from longer fibers, but they have greater ductility leading to a larger flexion during rubbing, reducing the depth of the surface grooves created on PIs. Therewith, the films surface mainly interacts with lateral side of the fiber than with its tip. Conversely, cotton velvet fibers even if they are shorter, they are rougher and penetrate better with the tip of the PI surface, generating more intense tracks. For all poly(oxadiazole-naphthylimide)s, a better regularity of surface topography is achieved when they are rubbed with V_{CD}. This observation might be ascribed to the longer constituent fibers that are better covering the films surface. In addition, its different chemical structure causes a different polymer-fiber interactions and implicitly different rearrangement of the polymer chains at the surface. The rubbing process determines fluctuations of electrons in

Table 3 The amplitude parameters calculated for the pristine and rubbed poly(oxadiazole-naphthylimide) films surfaces

Sample	Amplitude parameters	
	Skewness (Ssk)	Kurtosis (Sku)
PI1	0.203	15.755
PI2	0.101	5.228
PI3	0.068	3.620
PI4	2.635	13.617
PI1–V_C	−0.138	−0.263
PI2–V_C	−0.362	−0.074
PI3–V_C	−0.287	−0.064
PI4–V_C	−0.248	−0.109
PI1–V_{CD}	−0.025	−0.063
PI2–V_{CD}	−0.149	0.023
PI3–V_{CD}	−0.301	0.398
PI4–V_{CD}	−0.165	0.475

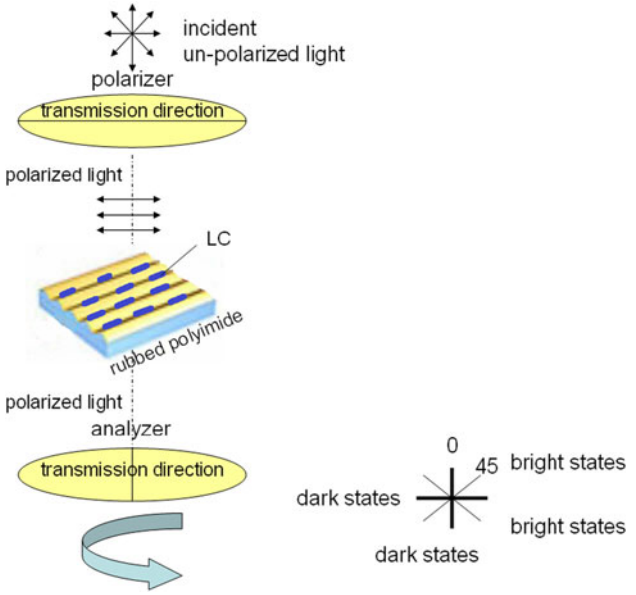

Scheme 2 The principle of testing the alignment of LC on patterned surface using the polarized light microscope

polar and nonpolar molecules giving rise to electrostatic interactions between the textile fibers and polymer surface. Also, hydrogen bonding might occur between the delocalized electrons from the ether linkages or N and O atoms from imide rings and hydroxyl groups from the fiber. The balance between the attractive and repulsive forces influences the AL surface regularity. Having all these in consideration, it can be stated that when patterning with V_C (with more polar hydroxyl groups than V_{CD}) higher repulsion forces between permanent dipoles (Keesom) are raised and their orientation direction is randomly distributed, excepting the fiber movement sense. Thus, local perturbations of the dipoles alignment lead to different arrangement of the chains and globally to surface pattern nonuniformity. Conversely, when using a less polar fiber (V_{CD}) the prevalent interactions consist in attractive dipoles dispersion and permanent dipoles-induced dipoles. These van der Waas forces are mainly following the rubbing direction of the fibers and this is reflected in a more uniform surface.

Testing of 5CB orientation ability

The mechanism of LC molecules orientation on rubbed polyimide depends on various factors including surface topography and intermolecular interactions. The factor which plays a major role is not fully understood. The LC alignment mechanism is determined by a combination between two effects: liquid crystal orientational elasticity in connection with an induced surface pattern [39] and short-range interactions on the molecular scale [42, 43]. Given the surface pattern PI films and the characteristics derived from their structure, the alignment mechanism can be included in both categories. There is a contribution of the imide rings to the intermolecular interactions of the PI with the 5CB molecules through the interactions with the polar carbonyl groups. In addition, according to the literature data [44], the ether linkages have partially polar character and might also interact with the LC molecules, resulting in a positive contribution to the LC alignment.

The alignment behavior of 5CB on poly(oxadiazole-naphthylimide)s PI1–PI4, rubbed with the two types of velvet, is tested by PLM. The principle of the method is based on recording the changes in light intensity when the sample (placed under crossed polarizers) is rotated 360°. For all films, dark regions are obtained at 0° and 90° rotation of the LC director with respect to the crossed polarizers, indicating it is aligned parallel to the polarizer transmission direction. By rotating the sample from this position at 45° and 135° with respect to the crossed polarizers, bright states are remarked because the electric field components passing through the easy direction of 5CB give the highest resultant on the analyzer transmission direction, as illustrated in Scheme 2. This behavior is characteristic for homogeneous alignment of a liquid crystal.

Considering the regularity of the created pattern it can be noticed that the higher uniformity of the surfaces rubbed with V_{CD} leads to higher contrast between the dark and bright states (as seen in Fig. 15). This is indicative that the 5CB alignment is more uniform in case of V_{CD}. The performance of alignment abilities are ranging in the following order: PI1 > PI4 > PI2 > PI3. Considering the transparency and surface morphology, it can be concluded

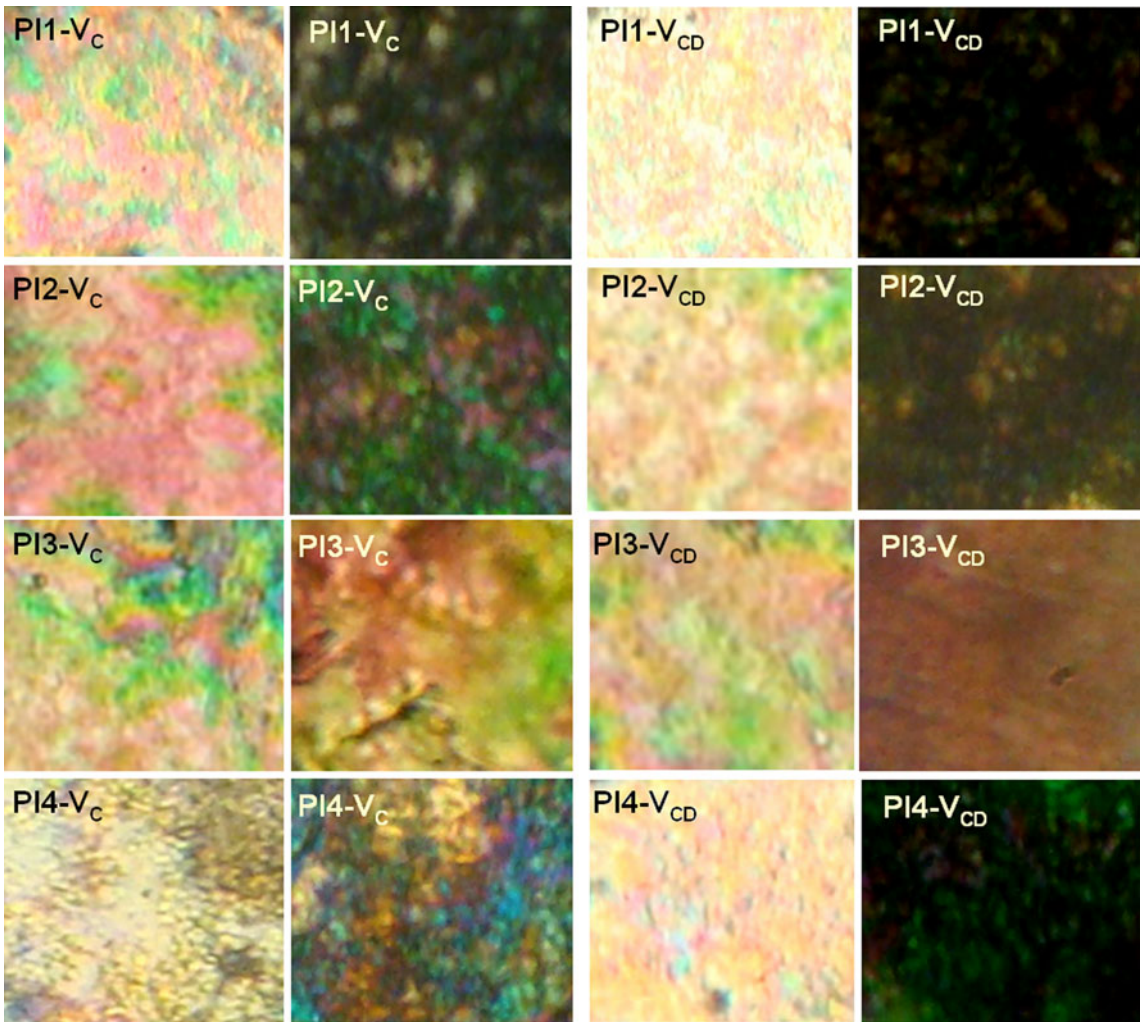

Fig. 15 PLM images revealing dark and bright states as result of 5CB orientation on patterned PI1–PI4 samples

that of all the PI films evaluated in the present work, PI1 which has the maximum tensile strength and elongation meet the requirements as AL for LCDs.

Conclusions

New rheological data of PIs-containing oxadiazole units and naphthalene rings in NMP solutions are reported in order to determine the proper films with adaptable morphology for LC orientation purposes. The optimum conditions for achieving mechanically resistant AL are determined by the PI chemical structure and molecular weight, which in turn are reflected in formation of chain entanglements. The entanglement concentration is evaluated from the dependence of specific viscosity on concentration. The effect of this type of chain interactions is detected in the flow behavior and consistency index. The presence of a small plateau in the shear moduli dependence on frequency also indicates that the formation of chain entanglements enhances the elastic components of the material. The elasticity of the samples determined in solution is in good agreement with the mechanical data for the corresponding films obtained in the semidilute entangled regime in Newtonian domain. All the PIs revealed good optical transparency, with a percentage of transmittance up to 89 % in the wavelength range of 400–700 nm. These polymers having oxadiazole-naphthylimide structures are processed into thin, flexible, and tough free-standing films having the thickness in the range of tens of micrometers. The morphology of the polyimide films, patterned with two types of velvet, is evaluated using AFM. Better regularity of PI surface is observed when rubbing with V_{CD} comparatively V_C. Analysis the Stdi values leads to the conclusion that minimum degree of entanglements is required for insuring the surface uniformity, but the dominate factor in surface orientation is PI chain flexibility. The effect of rubbing textile fiber on

alignment properties is tested with 5CB by PLM. The changes of the light intensity into dark and bright states obtained at 0° and 90° rotation of the LC director with respect to the crossed polarizers and at 45° and 135°, respectively, are indicative of uniform LC orientation, particularly when rubbing with V_{CD}. Therefore, these polymers having a six-member imide structure and oxadiazole moieties are promising candidates for applications as alignment layers in LCD devices, especially PI1 sample.

Acknowledgements This work was financially supported by PNII-RU project, code TE_221/2010, no. 31/10.08.2010.

References

1. Barzic AI, Stoica I, Hulubei C (2012) Semi-alicyclic polyimides: insights into optical properties and morphology patterning approaches for advanced technologies. In: Abadie MJM (ed) High performance polymers–polyimides based—from chemistry to applications. InTech, Novi Sad, pp 167–214
2. Tongsheng L, Peihong C, Xujun L, Jiang T, Qunji X (2000) Tribophysical and tribochemical effects of a thermoplastic polyimide. J Mater Sci 35:2597–2601. doi:10.1023/A:1004775331707
3. Ghosh MK, Mittal KL (1996) Polyimides: fundamentals and applications. Marker Dekker, New York
4. Chen JP, Labarthet FL, Natansohn A, Rochon P (1999) Highly stable optically induced birefringence and holographic surface gratings on a new azocarbazole-based polyimide. Macromolecules 32:8572–8579
5. Garcia JM, Garcia F, Sanz R, de la Campa JG, Lozano AE, de Abajo J (2001) Synthesis and characterization of new soluble polyamides derived from 2,6-bis(4-aminophenyl)-3,5-dimethyltetrahydro-4H-pyran-4-one. J Polym Sci A 39:1825–1832
6. Staubli A, Mathiowitz E, Langer R (1991) Sequence distribution and its effect on glass transition temperatures of poly(anhydride-co-imides) containing asymmetric monomers. Macromolecules 24:2291–2298
7. Damaceanu MD, Rusu RD, Bruma M (2012) Six-member polyimides incorporating redox chromophores. J Mater Sci 47:6179–6188. doi:10.1007/s10853-012-6542-8
8. Pasahan A, Koytepe S, Ekinci E (2011) Synthesis, characterization of naphthalene-based polyimides, and their use as immobilized enzyme membrane. Polym Adv Technol 22:1940–1947
9. Damaceanu MD, Rusu RD, Nicolescu A, Bruma M (2011) Blue fluorescent polyamides containing naphthalene and oxadiazole rings. J Polym Sci A 49:893–906
10. Damaceanu MD, Rusu RD, Bruma M, Rusanov A (2010) Fluorinated heterocyclic polyperyleneimides. Rev Roum Chim 55:953–961
11. Kizhnyaev VN, Pokatilov FA, Vereshchagin LI (2008) Carbochain polymers with oxadiazole, triazole, and tetrazole cycles. Polym Sci Ser C 50:1–21
12. Kim SW, Shim SC, Jung BJ, Shim HK (2002) Synthesis and properties of new electroluminescent polymers possessing both hole and electron-transporting units in the main chain. Polymer 43:4297–4305
13. Liu JG, He MH, Zhou HW, Qian ZG, Wang FS, Yan SYJ (2002) Organosoluble and transparent polyimides derived from alicyclic dianhydride and aromatic diamines. Polym Sci A 40:110–119
14. Hahm SG, Lee TJ, Chang T, Jung JC, Zin WC, Ree M (2006) Unusual alignment of liquid crystals on rubbed films of polyimides with fluorenyl side groups. Macromolecules 39:5385–5392
15. Takatoh K, Hasegawa M, Koden M, Itoh N, Hasegawa R, Sakamoto M (2005) Alignment technologies and applications of liquid crystal devices. Taylor & Francis, London
16. Hirosawa I, Koganezawa T, Ishii H, Sakai T (2009) Effects of annealing on rubbed polyimide surface studied by grazing-incidence X-ray diffraction. IEICE Trans Electron E92C:1376–1381
17. Hirosawa I, Sasaki N, Kimura H (1999) Characterization of molecular orientation of rubbed polyimide film by grazing incidence X-ray scattering. Jpn J Appl Phys 38:L583–L585
18. Uchida T, Seki H (1992) Liquid crystals: applications and uses. World Scientific, Singapore
19. Barzic AI, Stoica I, Popovici D, Vlad S, Cozan V, Hulubei C (2013) An insight on the effect of rubbing textile fiber on morphology of some semi-alicyclic polyimides for liquid crystal orientation. Polym Bull 70:1553–1574
20. Geary JM, Goodby JW, Kemtz AR, Patel JS (1987) The mechanism of polymer alignment of liquid crystal materials. J Appl Phys 62:4100–4108
21. Damaceanu MD, Rusu RD, Bruma M, Jarzabek B (2010) Photooptical properties of poly(oxadiazole-imide)s containing naphthalene rings. Polym J 42:663–669
22. Damaceanu MD, Rusu RD, Bruma M, Rusanov AL (2011) New thermally stable and organosoluble heterocyclic poly(naphthaleneimide)s. Polym Adv Technol 22:420–429
23. Rusu RD, Damaceanu MD, Bruma M, Ronova IA (2011) Effect of conformational parameters on thermal properties of some poly(oxadiazole-naphthylimide)s. Iran Polym J 20:29–40
24. Han Y, Fang XZ, Zuo XX (2010) The influence of molecular weight on properties of melt-processable copolyimides derived from thioetherdiphthalic anhydride isomers. J Mater Sci 45:1921–1929. doi:10.1007/s10853-009-4179-z
25. Teraoka I (2002) Polymer solutions: an introduction to physical properties. Wiley, New York
26. Krause WE, Bellomo EG, Colby RH (2001) Rheology of sodium hyaluronate under physiological conditions. Biomacromolecules 2:65–69
27. Bordi F, Colby RH, Cametti C, De Lorenzo L, Gili TJ (2002) Electrical conductivity of polyelectrolyte solutions in the semidilute and concentrated regime: the role of counterion condensation. J Phys Chem B 106:6887–6893
28. de Gennes PG (1979) Scaling concepts in polymer physics. Cornell University Pres, New York
29. Jenekhe SA (1983) The rheology and spin coating of polyimide solutions. Polym Eng Sci 23:830–834
30. Britten JA, Thomas IM (1992) Non-Newtonian flow effects during spin coating large-area optical coatings with colloidal suspensions. J Appl Phys 71:972–979
31. Gutzow I, Dobreva A, Schmelzer J (1993) Rheology of non-Newtonian glass-forming melts. J Mater Sci 28:901–908. doi:10.1007/BF00400872
32. Rennie TJ, Vijaya Raghavan GS (2007) Thermally dependent viscosity and non-Newtonian flow in a double-pipe helical heat exchanger. Appl Therm Eng 27:862–868
33. McNally T, McShane P, Nally GM, Murphy WR, Cook M, Miller A (2002) Rheology, phase morphology, mechanical, impact and thermal properties of polypropylene/metallocene catalysed ethylene 1-octene copolymer blends. Polymer 43:3785–3793
34. Cosutchi AI, Hulubei C, Ioan S (2007) Rheological study of some epiclon-based polyimides. J Macromol Sci B 46:1003–1012
35. Chisca S, Barzic AI, Sava I, Olaru N, Bruma M (2012) Morphological and rheological insights on polyimide chain entanglements for electrospinning produced fibers. J Phys Chem B 116:9082–9088
36. Cole KS, Cole RH (1941) Dispersion and absorption in dielectrics I. Alternating current characteristics. J Chem Phys 9:341–351

37. Harrell ER, Nakayama N (1984) Modified cole–cole plot based on viscoelastic properties for characterizing molecular architecture of elastomers. J Appl Polym Sci 29:995–1010
38. Cosutchi AI, Hulubei C, Stoica I, Dobromir M, Ioan S (2008) Structural and dielectric properties of some epiclon-based polyimide films. e-Polymers 8:778–792
39. Berreman DW (1973) Alignment of liquid crystals by grooved surfaces. Mol Cryst Liq Cryst 23:215–231
40. Murata M, Yoshida E, Uekita M, Tawada Y (1993) Effect molecular arrangement of alignment film for liquid crystals. Jpn J Appl Phys 32:L676–L678
41. Lee SW, Lee SJ, Hahm SG, Lee TJ, Lee B, Chae B, Seung BK, Jin CJ, Wang CZ, Byeong HS, Moonhor R (2005) Role of the n-alkyl end of bristles in governing liquid crystal alignment at rubbed films of brush polymer rods. Macromolecules 38: 4331–4338
42. Johannsmann D, Zhou H (1993) Correlation between surface and bulk orientations of liquid crystals on rubbed polymer surfaces: odd–even effects of polymer spacer units. Phys Rev E 48:1889–1896
43. Kikuchi H, Logan JA, Yoon DY (1996) Study of local stress, morphology, and liquid–crystal alignment on buffed polyimide surfaces. J Appl Phys 79:6811–6817
44. Chae B, Kim SB, Lee SW, Kim SI, Choi W, Lee B, Ree M, Lee KH, Jung JC (2002) Surface morphology, molecular reorientation, and liquid crystal alignment properties of rubbed nanofilms of a well-defined brush polyimide with a fully rodlike backbone. Macromolecules 35:10119–10130